Title
Thermomechanical Responses of Thermally Interacting Field-Scale Energy Piles

Journal
International Journal of Geomechanics, 22(11)

ISSN
1532-3641

Authors
Moradshahi, Aria
Faizal, Mohammed
Bouazza, Abdelmalek
et al.

Publication Date
2022-11-01

DOI
10.1061/(asce)gm.1943-5622.0002523

Peer reviewed

Thermo-mechanical responses of thermally interacting field-scale energy piles

Aria Moradshahi

PhD student, Monash University, Department of Civil Engineering, 23 College Walk, Clayton, Vic. 3800, Australia. Telephone: +61 3 990 58901; Email: aria.moradshahi@monash.edu

Mohammed Faizal

Research Fellow, Monash University, Department of Civil Engineering, 23 College Walk, Clayton, Vic. 3800, Australia. Telephone: +61 3 9902 9988; Email: mohammed.faizal@monash.edu

*** Abdelmalek Bouazza (Corresponding Author)**

Professor, Monash University, Department of Civil Engineering, 23 College Walk, Clayton, Vic. 3800, Australia. Telephone: +61 3 9905 4956; Email: malek.bouazza@monash.edu

John S. McCartney

Professor and Department Chair, University of California San Diego, Department of Structural Engineering, 9500 Gilman Drive, SME 442J, La Jolla, CA 92093-0085, USA, Telephone: +1 858 534 9630; Email: mccartney@ucsd.edu

Abstract

Energy piles have great potential for improving the heating and cooling performance of new buildings. However, their axial and radial thermo-mechanical behaviour due to thermal interaction between different energy piles through the surrounding soil is not well understood. This paper combines results from field experiments and numerical simulations on two bored energy piles with a centre-to-centre spacing of 3.5 m to investigate how energy piles interact under balanced and imbalanced daily temperature cycles and a range of monotonic thermal loads. One of the two energy piles' axial and radial thermo-mechanical responses were investigated during single and dual pile operation. Cyclic temperature variations of the piles induced lower soil temperature changes and pile thermal stresses than monotonic temperature variations. The balanced cyclic temperatures induced lower thermal effects in the pile and the soil than imbalanced cyclic temperatures. Significant soil temperature changes were recorded between the piles when the two piles were heated to 40°C and cooled to 0°C. However, the pile thermal stresses were similar for single and dual pile operations, indicating that thermal interaction between the piles through the surrounding soil had negligible effects on pile behaviour for the setting investigated in this paper. The piles radial thermal stresses were negligible compared to the axial thermal stresses for all studied cases. Overall, the results from this study provide validated insights into the situations where thermal interaction should be considered in design.

Keywords: *Energy piles; field tests; thermal interaction; temperature cycles.*

Introduction

Multiple energy piles are commonly installed within a building footprint to help meet its structural demand and indoor heating and cooling requirements. The thermal interaction between closely spaced energy piles through the soil may influence the piles' axial and radial thermo-mechanical behaviour. While other studies have investigated thermal interaction between energy piles in a group, there are still remaining questions about the roles of heating-cooling cycles versus monotonic heating on the pile stress-strain response, and how heat transfer between the piles in these two heat transfer modes affects transient energy pile behavior. The magnitudes of fluid temperatures entering the energy piles from the exit of the ground source heat pump (GSHP) is the key deciding factor on the magnitudes of thermal effects in the piles and the soil, so it is critical to understand in the energy pile group design.

Thermal interaction between closely spaced energy piles in a group has been investigated in several studies during monotonic thermal loading, primarily through the mechanical link connecting the piles such as a raft or a cap (Jeong et al. 2014; Mimouni and Laloui 2015; Salciarini et al. 2015; Di Donna et al. 2016; Saggu and Chakraborty 2016; Rotta Loria and Laloui 2016, 2017a, 2017b, 2018; Salciarini et al. 2017; Ravera et al. 2019; Fang et al. 2020; Wu et al. 2020). These studies mainly evaluated the axial thermal stresses, while only few evaluated changes in radial thermal stresses (Mimouni and Laloui 2015; Moradshahi et al. 2020a). These previous studies have not considered the influence of different magnitudes of monotonic and cyclic thermal loads on the thermo-mechanical behaviour of the piles due to temperature variations of the soil volume between the piles. Cyclic thermal loading may involve a faster rate of heating and cooling that may not heat the soil between the energy piles as much as the case of monotonic heating, so less thermo-mechanical interaction could be expected.

A number of studies have evaluated the thermal responses of solitary energy piles subjected to monotonic temperatures (e.g. Laloui et al. 2006; Bourne-Webb et al. 2009; Akrouch et al. 2014; Mimouni 2014; Murphy and McCartney 2015; Wang et al. 2015; Murphy et al. 2015; Sutman et al. 2015; Khosravi et al. 2016; Adinolfi et al. 2018; Anongphouthet al. 2018; Rui and Soga 2018; Sung et al. 2018; Faizal et al. 2019a; Liu et al. 2019; Moradshahi et al. 2020b) and cyclic temperatures (e.g. Abdelaziz and Ozudogru 2016; Faizal et al. 2016; Ng and Gunawan 2016; Suryatriyastuti et al. 2016; Faizal et al. 2018, 2019b; Sung et al. 2018; Huang et al. 2018; Sarma and Saggu 2020; Yang et al. 2020). Compared to monotonic temperatures, cyclic temperatures induce lower ground temperature changes and lower thermal stresses in solitary energy piles (Faizal et al., 2016, 2018, 2019b). Therefore, it can be hypothesised that cyclic thermal loading of energy piles would also reduce the thermal stresses in multiple energy piles and reduce the thermal interaction through the soil volume between the piles. Moreover, depending on the daily operating to rest time ratios of the ground source heat pump, the piles and the ground could experience daily balanced or imbalanced cyclic thermal loads (Olgun et al. 2015), which could also affect the thermo-mechanical behaviour of thermally interacting energy piles.

The magnitudes of thermal stresses in the piles and the zone of radial thermal influence in the soil depend on the magnitude of the inlet fluid temperatures entering the energy piles from the ground source heat pump. Previous results from solitary energy pile investigations subjected to monotonic temperature variations have indicated that the soil temperature changes are largest near the pile and reduce with increasing radial distance from the pile (e.g. Li et al. 2006; Bourne-Webb et al. 2009; You et al. 2014; Singh et al. 2015; Yu et al. 2015; Faizal and Bouazza 2018; Guo et al. 2018; Murphy et al. 2015; Chen et al. 2017). The soils radial thermal influence zones of individual piles can overlap with the radial thermal zone of nearby piles (i.e. thermal interaction between the piles). They can cause an overall increase or decrease of the soil temperatures between the piles, as indicated in a few field tests under monotonic temperatures (You et al., 2014; Moradshahi et al., 2020a). Therefore, varying inlet fluid temperatures and temperature cycles can be hypothesised to influence the piles' thermal interaction through the soil volume, which could affect the axial and radial thermal responses of the piles.

This paper investigates the hypotheses mentioned earlier by correlating field and numerical methods on two energy piles installed beneath a six-storey residential building. The soil temperature variations between the piles and the axial and radial thermo-mechanical responses of one of the two energy piles are investigated during single and dual pile operation. Investigations are conducted for a range of typical monotonic heating and cooling temperatures and balanced and imbalanced cyclic temperatures. These different magnitudes of inlet fluid temperatures are selected to represent a wide range of temperatures experienced by the piles at different installation sites.

Experimental procedure

Two energy piles were installed under a six-storey residential building in the Brighton Group of materials, which are dense to very dense clayey sands as described by Barry-Macaulay et al. (2013) and Faizal et al. (2018, 2019a, 2019b). The piles had a diameter of 0.6 m and length of 10 m and were spaced at a centre-to-centre distance of 3.5 m. A schematic of the piles is shown in Figure 1. Four U-shaped heat exchanger loops made with high-density polyethylene (HDPE) pipes were attached to the reinforcing cages up to the depth of both piles. One of the two piles (EP1) is instrumented with axial and radial vibrating wire strain gauges (Model: Geokon-4200) at five depths. The compressive strength and elastic modulus of unreinforced concrete cylindrical samples measured in the laboratory were 64 MPa and 34 GPa, respectively. The water temperatures and flow rates at the inlet and outlet of the U-loops were recorded by Type T thermocouples and TM-series digital water flow meters, respectively. The ground temperatures were recorded using Type T thermocouples at two 12 m deep boreholes between the two piles (Figure 1). A detailed description of the two piles is given in Faizal et al. (2019a and 2019b).

The piles were subjected to monotonic heating, monotonic cooling, and daily cyclic heating/cooling temperatures. Six field tests were conducted in total, where the instrumented pile (EP1) was tested alone and simultaneously with the second pile (EP1 + EP2). The inlet water temperatures for each experiment is shown in Figure 2, and the details of the experiments are given in Table 2. There were difficulties in controlling the fluid temperatures between single and dual pile temperatures, most likely due to the additional length of pipes in dual-pipe experiments compared to single pile experiments. The sudden increase in inlet fluid temperature on day 4 of the dual pile heating experiment was due to switching on an additional heating element to increase the inlet fluid temperature. There were also some performance issues with the heat pump during dual pile cooling and cyclic operations, which affected the inlet fluid temperature trends. The heating and cyclic temperature data for the single pile operation was obtained from Faizal et al. (2019a, 2019b).

Numerical modelling

Numerical modelling was conducted to supplement the field data by simulating various magnitudes of inlet fluid temperatures. The three-dimensional finite element numerical model used in this paper was developed by Moradshahi et al. (2020a) using the COMSOL Multiphysics software. The model was validated using field data, i.e. inlet fluid temperatures, ground temperature changes, temperatures of EP1, and axial and radial thermal strains/stresses of EP1. The complete details of the model are provided in Moradshahi et al. (2020a).

The 40 × 15 × 30 m^3 3D finite element model, shown in Figure 3, consisted of 344821 tetrahedral, triangular, prismatic, linear and vertex elements. The roller boundary conditions were applied to the sides of the numerical model to allow vertical movements. The bottom boundary was fully mechanically restricted, whereas the top boundary was considered a free boundary. The ground and pipe temperatures were set to 15°C, which is the average ground temperature. No interface element was assumed for the soil-pile interface, and the energy piles and the soil were considered to be perfectly bonded to each other at the pile-soil interface. Similar assumptions were made in recent numerical studies (e.g. Batini et al., 2015; Gawecka et al., 2017; Rotta Loria and Laloui, 2017b, 2018; Salciarini, 2017; Adinolfi et al., 2018; Liu et al., 2020).

Each energy pile was connected to a separate slab with a dimension of 5 × 5 × 0.5 m (length × width × height). There was no groundwater encountered within the depth of the pile, and the soil at the site was considered to be dry. The soil, energy piles, and slab thermal and mechanical properties used in the numerical model were selected based on previous studies conducted on the same field test site (Barry-Macaulay et al., 2013; Singh et al., 2015; Faizal et al., 2018, 2019) and from common properties reported in the literature (Bowles 1968; Peck et al., 1974; Mitchell and Soga, 2005; Bourne-Webb et al., 2009; Amatya et al., 2012, Singh and Bouazza, 2013). A working load of 1400 kN was applied at the surface of the slabs above the two piles heads to simulate the building loads (Faizal et al., 2019).

The numerical analysis of the thermo-mechanical response of the energy piles is based on the following assumptions: (a) the energy piles and slabs were considered to be isotropic, elastic materials; (b) the solid is considered to be incompressible under isothermal conditions; (c) the inertial effects of the solid skeleton are negligible, and the simulations represent quasi-static conditions; (d) a Mohr-Coulomb model governed by a non-associated flow rule was used for the ground surrounding the energy pile; and (e) the soil was assumed to be dry and heat transfer was considered to be purely conductive. The governing equations used to develop the model are given in detail in Moradshahi et al. (2020) although the model was modified to include the Mohr-Coulomb model to capture more realistic behaviour of the soil under temperature cycles.

Validation of the numerical model

The field and numerical results for monotonic and cyclic temperature operations, respectively, at the end of each experiment for single and dual pile operation, are shown in Figure 4. For cyclic operations, the results are presented at the end of heating and end of cooling for the last cycle of each experiment. The numerical results for the axial and radial thermal strains and stresses were derived at the pile centre in the numerical model. The radial contact stresses were, however, obtained at the pile-soil interface. Positive and negative signs indicate tensile and compressive stresses, respectively. The experimental strains were measured using vibrating wire strain gauges as detailed in Faizal et al. (2019a). The following equation was used to obtain the experimental axial thermal stresses in EP1:

$$\sigma_T = E_P(\varepsilon_{obs} - \alpha_{free}\Delta T) \quad (1)$$

where E_P is the elastic modulus of the concrete (taken as 34 GPa), ε_{obs} is experimentally observed thermal strain, α_{free} is the free thermal expansion coefficient of the concrete (taken as 13 με/°C), and ΔT is the change in temperature of the pile.

A cavity expansion analysis was used to estimate the experimental radial thermal stresses in the pile as follows:

$$\sigma_n = \frac{E_s \Delta r}{(1 + v_s) r} \quad (2)$$

where E_s and v_s are the elastic modulus and Poisson's ratio of the surrounding sand, respectively, which are assumed to be 60 MPa and 0.3, respectively, based on typical values for dense sand (Faizal et al. 2019; Elzeiny et al., 2020), r is the radius of EP1, and Δr is the thermally induced radial displacement of EP1.

The changes in temperature of EP1 for single and dual pile operations, as shown in Figures 4a and 4b, are almost uniform with depth for all operations. Due to differences in inlet fluid temperatures between experiments, primarily for cyclic operations (Figure 2b), the changes in pile temperatures are different for the cyclic experiments, as shown in Figure 4b. The changes in ground temperature with increasing radial distance from the sides of EP1 and EP2 for a depth of 5 m for monotonic and cyclic operations, respectively, are shown in Figures 4c and 4d. A depth of 5 m was selected because it is at the mid-depth of the pile where thermal effects from the pile ends are likely negligible. Due to the radial overlap of ground temperatures resulting from simultaneous operation of energy piles, dual pile operation induced higher ground temperatures between the two energy piles. However, cyclic temperatures caused lower ground temperature changes than monotonic temperatures for both single and dual pile operations due to frequent recovery of the ground temperatures.

The lowest and highest values of axial thermal strains and stresses were observed at a depth of around 2.6 m for monotonic operations (Figures 4e and 4i). This depth represents the location of the null point, which can be attributed to the higher stiffness of the upper soil layers and overlying structure. The radial thermal strains in all operations (Figures 4g and 4h) are generally higher than axial thermal strains, indicating lower thermal expansion/contraction restriction in the radial direction. The radial thermal stresses in EP1 (Figures 4k and 4l) were significantly lower than the axial thermal stresses (Figures 4i and 4j) for all cases. The discrepancies in numerical results, especially around the depth of 7 m, can be attributed to the assumptions and limitations in the numerical model, such as assuming a linear elastic – perfectly plastic with constant stiffness of the soil for each layer.

Parametric investigations

The validated numerical model was used to assess the effect of varying inlet fluid temperatures on the thermal responses of EP1. Four inlet fluid temperatures were studied for heating and cooling monotonic temperatures and three for cyclic temperatures, as shown in Figure 5a. The initial fluid temperature was set to 20°C at the beginning of all tests, close to the average initial ground temperature. The fluid temperatures were varied by ± 5°C intervals for monotonic temperatures (i.e. $|\Delta T_f|$ = 5°C, 10°C, 15°C, 20°C, where ΔT_f is the difference between the inlet fluid temperatures and the initial fluid temperature of 20°C).

Three patterns of cyclic daily temperatures were simulated, representing an intermittent operation of the GSHP, as shown in Figures 5b to 5d. First, balanced cyclic temperatures with 12 hours heating and 12 hours cooling between 10°C and 30°C (referred to as balanced cyclic in Figure 5b). Second, imbalanced cyclic temperatures inclined towards heating, with 16 hours heating and 8 hours cooling. The minimum and maximum temperatures were 10°C and 40°C, respectively. Third, imbalanced cyclic temperatures inclined towards cooling, with 8 hours heating and 16 hours cooling. The maximum and minimum temperatures were 30°C and 0°C, respectively. These daily cyclic temperatures were purposefully selected to represent a higher order of temperatures simulating extreme cases such as forced recharging from additional heaters such as solar panels.

It was assumed that the two energy piles were working separately in the numerical analysis (i.e. heat exchanger pipes are not connected in series) with the same inlet fluid temperatures (shown in Figure 5) and same fluid flow rate of 11 L/min. In this way, both EP1 and EP2 have the same rate of heating or cooling. This assumption is appropriate for this paper since only the thermo-mechanical responses of EP1 are analysed. Also, the initial pile and ground temperatures were assumed to be the same for all simulations to isolate better and investigate the effects of varying fluid temperatures. The results are presented for the last day of operation (Day 18). Conducting these tests at a field scale would be time-consuming, expensive, and difficult to maintain the same boundary conditions for all experiments; hence the numerical approach in this paper provides valuable insights since the model was developed using the field data.

Results and discussions

Pile and ground temperatures

The effect of fluid temperature variations on temperatures and change in temperatures in EP1 is shown in Figure 6 for all simulations. The pile temperatures increased with increasing magnitudes of inlet fluid temperatures, with relatively uniform profiles with depth for all cases. Cyclic fluid temperatures induced lower pile temperatures in EP1. The change in EP1 temperatures varied between -19 ºC to 18 ºC for monotonic temperatures (Figure 6b) and between -12.5 ºC to 11ºC for cyclic temperatures (Figures 6c and 6d). Also, the balanced cyclic temperatures imposed lower temperatures compared to the other two imbalanced cyclic temperatures. There were no significant differences in EP1 temperatures for single and dual pile operation for all tests, indicating that the operation of EP2 did not affect the temperatures of EP1 and the effect of thermal interaction through the soil between the piles was negligible on pile temperatures for the spacing investigated in this study.

The effect of fluid temperature variations on change in ground temperatures between the two energy piles at a depth of 5 m (mid-depth of the pile where pile ends thermal effects are likely negligible) is shown in Figure 7 for both single and dual pile operation. For any given operation mode, ground temperature changes increased with increasing absolute fluid temperatures for both single and dual pile operation. For the operation of EP1 alone and any given fluid temperature, the changes in ground temperatures were highest near EP1 and reduced with increasing radial distance from the edge of EP1. For a single energy pile operation, the soil's zone of radial thermal influence increased with increasing absolute fluid temperatures.

During dual pile operation, for any given fluid temperature, the ground temperatures initially reduced with increasing radial distance from the edges of the two piles but overlapped between the two piles and induced greater changes in ground temperatures compared to single pile operation. The effect of cyclic temperature variations on ground temperature changes (with the maximum temperature change of 7°C for heating oriented cyclic temperatures) is significantly lower than monotonic temperatures (with the maximum temperature change of 13°C for both monotonic heating and cooling), for both single and dual pile operation. A similar observation was reported by Faizal et al. (2016), where lower ground temperatures were observed for the cyclic operation of a solitary energy pile. The lowest change in ground temperature of 2.5°C was observed for the balanced cyclic operation (Figure 7c). Cyclic temperatures, particularly the balanced cyclic temperatures, would induce lower ground temperatures and thermal interaction between the piles through the soil compared to monotonic temperatures for long-term operations.

Axial and radial thermal strains and stresses of EP1

The effect of fluid temperature on the axial thermal strains and stresses of EP1 is shown in Figure 8. The thermal strains and stresses increased with the increasing absolute value of inlet fluid temperatures for single and dual pile operations. The maximum axial thermal stresses' location remained at approximately 3 m depth for all the cases due to the considerable stiffness of the building on the pile head, which indicates the location of the null point is independent of magnitudes of inlet fluid temperature for the current in-situ conditions.

The strains and stresses of EP1 were similar for single and dual pile operation with slight differences in the upper pile section for all fluid temperatures, indicating that the operation of EP2 during dual pile operation did not influence the thermal response of EP1 even though the ground temperature changes were greater during dual pile operation (Figure 7). A similar observation was reported by Moradshahi et al. (2020a) for the same energy pile setup and given fluid temperatures for different soil parameters. However, in the previous studies on the group of energy piles (Jeong et al., 2014; Mimouni and Laloui 2015; Rotta Loria and Laloui 2017b and 2018), where the energy piles were linked mechanically with a slab or raft, the effect of the operating energy pile on the nearby energy pile were more significant for given inlet fluid temperatures; specifically, for the upper parts of the energy piles due to the slab deformation. In the present study, the maximum axial thermal stresses were -4.2 MPa and 3.5 MPa for monotonic heating and monotonic cooling, respectively (Figures 8b and 8d). Due to lower temperature changes, cyclic operations induced lower axial thermal strains and stresses in EP1 than monotonic temperatures, with the maximum thermal stresses ranging between -3.4 – 3.2 MPa for imbalanced heating and imbalanced cooling, respectively, at a depth of 2.6 m (Figure 8f). However, these magnitudes were as low as 1.2 MPa for balanced cyclic operation.

The effect of fluid temperature on the radial thermal responses of EP1 is shown in Figure 9. Higher inlet fluid temperatures induced higher radial thermal strains and stresses in EP1 for single and dual-pile operation. However, the radial thermal stresses were significantly lower than the magnitudes of axial thermal stresses for all tests, consistent with other studies' findings (Ozudogru et al., 2015; Gawecka et al., 2017; Faizal et al., 2018, 2019). Similar to the axial thermal responses, the radial thermal stresses in EP1 was not significantly affected by the operation of EP2 during dual pile operation, which further confirms the negligible effects of the operation of one energy pile on the other nearby energy pile due to thermal interaction through the soil volume for the pile spacing investigated in this study. The three cyclic temperature modes generated lower radial thermal stresses ranging between -6 kPa to 6 kPa in EP1 for both single and dual pile operations compared to monotonic temperatures with values of -22 kPa and 10 kPa for monotonic heating and monotonic cooling, respectively. Moreover, higher magnitudes of radial thermal stresses were observed for imbalanced cyclic temperature variations than balanced cyclic operations.

Axial and radial thermal displacements of EP1

The effect of varying fluid temperature on the axial and radial thermal displacements of EP1 for all monotonic and cyclic operations is shown in Figures 10. Positive and negative values of displacement mean upward and downward movements of EP1, respectively. The radial thermal displacements (Figures 10b, 10d, and 10f) were very low compared to axial thermal displacements (Figures 10a, 10c, and 10e) and ranged between -0.05 mm to 0.02 mm, for all tests. The axial thermal displacements at the pile head (ranged between -0.6 mm to 0.6 mm) were lower than near the toe (ranged between -1.2 mm to 1.2 mm) due to the higher restriction imposed by the building loads and higher stiffness of soil layers at the upper part of EP1 (Table 1). There were no significant differences between the displacements of EP1 in single and dual pile operations, indicating that the operation of the second pile in dual pile operation did not affect the displacements of EP1.

Increasing inlet fluid temperature increased the magnitudes of thermal displacements of EP1 for both single and dual pile operations. The maximum thermal axial displacement for monotonic temperatures was between -1.2 mm to 1.2 mm. However, cyclic temperatures had lower axial thermal displacements than monotonic temperatures, particularly for the balanced cyclic temperatures; the maximum axial thermal displacements were between -0.1 and 0.1 mm. The imbalanced cyclic operations had higher axial displacements than balanced cyclic temperatures (between -0.8 and 0.3 mm for imbalanced cyclic heating and between -0.3 and

0.8 mm for imbalanced cyclic cooling). The range of thermally induced displacements at the pile's head is consistent with the data available in the literature (Suryatriyastuti et al., 2012; Han and Yu 2020; Moradshahi et al., 2020a), and the results of this study show that the maximum pile's displacement even for extreme operations will not result in structural failure of the pile.

Thermal strains of EP1 versus change in pile temperature

The axial and radial thermal strains of EP1 against change in pile temperatures of EP1 were plotted (Figure 11) for all cases to compare the temperature-dependent responses of the pile for different inlet fluid temperatures for both single and dual pile operations. The results are presented for a depth of 2.6 m, which is the location of the null point, where the lowest thermal strains and highest thermal stresses were observed. For any given simulation (i.e. for either monotonic or cyclic temperatures and single or dual pile operations), the change in axial and radial thermal strains against change in pile temperatures was between 6.67 – 7.88 με/°C and 11.6 – 13 με/°C, respectively. This confirms that the axial thermal strains of EP1 had higher restrictions on thermal expansion/contraction compared to radial thermal strains.

For a given simulation, there were negligible differences in the change in thermal strains (for either axial or radial thermal strains) against change in pile temperatures between the single and dual pile tests, confirming that the operation of EP2 had negligible effects on the thermal responses of EP1. Linear responses for axial and radial thermal strains against changes in pile temperatures were observed for monotonic heating and cooling temperatures (Figures 11a and 11b). The thermal strains showed cyclic changes with respect to cyclic changes in pile temperatures (Figures 11c to 11f); however, the trends were linear with similar slopes to that of the monotonic temperature tests. The similarity in slopes between monotonic and cyclic temperature tests indicate that the cyclic temperature variations did not lead to unexpected plastic deformations for the range of temperatures, types of piles and soil conditions investigated in the current study.

The axial and radial thermal strains followed a reversible cyclic path between a constant range of change in pile temperature of -4 to 4 ºC in the balanced cyclic temperature tests for both single and dual pile tests (Figures 11c and 11d). There was a slight ratcheting behaviour for the first few cycles in the balanced cyclic temperature tests, which can be related to unstable pile temperatures at the beginning of the simulation (Figures 11c and 11d). For the imbalanced heating and cooling modes (Figures 11e to 11h), the range of change in pile temperatures variation led to irreversible responses of the thermal strains; the responses of thermal strains can, therefore, be inferred as being temperature-dependent and were not due to plastic deformations of the pile and the soil.

Conclusions

This paper investigated the axial and radial thermal responses of one of two field-scale energy piles spaced at a centre-to-centre distance of 3.5 m under monotonic and cyclic temperature changes, numerically and experimentally. The ground temperature changes between the energy piles were noticeably affected by the operation of the second energy pile, especially for monotonic temperatures with higher inlet fluid temperatures. The influence of the second energy pile on the magnitudes of temperature, axial and radial stresses and strains of the considered energy pile was, however, negligible, indicating that the influence of thermal interaction between the energy piles through the soil volume on the pile thermal responses was insignificant for the pile spacing and operation time considered in this study.

Higher values of axial thermal stresses developed in the considered energy pile during monotonic heating and cooling operations compared to cyclic operations for both single and dual pile tests were due to more significant changes in pile temperature. The thermal strains of the considered energy pile followed linear paths during monotonic and cyclic operations for both single and dual piles operations, indicating no plastic deformations for different magnitudes of monotonic and cyclic temperatures. The rates of change in thermal strains against change in pile temperatures for the considered energy pile were similar for both single and dual pile operations, indicating negligible effects of thermal interaction between the piles through the soil on the pile thermal responses for the conditions investigated in this paper. The outcomes of this paper can be considered in the design of closely spaced energy piles that interact thermally through the soil for a range of inlet fluid temperatures that energy piles might encounter.

Acknowledgements

This research project was supported under the Australian Research Council's Linkage Projects funding scheme (project number LP120200613). The authors also acknowledge the Australian Government Research Training Program Scholarship provided to the first author. The US National Science Foundation grant CMMI-0928159 supported the fourth author. The support of all the sponsors (Geotechnical Engineering-Acciona, Golder Associates, Geoexchange Australia, Brookfield-Multiplex) is gratefully acknowledged.

References

Akrouch, G., Sánchez, M., and Briaud, J-L. 2014. Thermo-mechanical behavior of energy piles in high plasticity clays. Acta Geotechnica, **9**(3): 399-412. https://doi.org/10.1007/s11440-014-0312-5.

Adinolfi, M., Maiorano, R. M. S., Mauro, A., Massarotti, N., and Aversa, S. 2018. On the influence of thermal cycles on the yearly performance of an energy pile. Geomechanics for Energy and the Environment, 16, 32-44. https://doi.org/10.1016/j.gete.2018.03.004.

Amatya, B.L., Soga K., Bourne-Webb P.J. 2012. Thermo-mechanical behaviour of energy piles. Géotechnique, **62**(6):503-519. https://doi.org/10.1680/geot.10.P.116.

Anongphouth, A., Maghoul, P. and Alfaro, M. 2018. Numerical Modeling of Concrete Energy Piles Using a Coupled Thermo-Hydro-Mechanical Model. In: 71st Canadian Geotechnical Conference, Edmonton, Alberta, Canada.

Batini, N., Loria, A. F. R., Conti, P., Testi, D., Grassi, W., and Laloui, L. 2015. Energy and geotechnical behaviour of energy piles for different design solutions. Applied Thermal Engineering, **86**: 199-213. https://doi.org/10.1016/j.applthermaleng.2015.04.050.

Bourne-Webb, P.J., B. Amatya, K. Soga, T. Amis, C. Davidson, and P. Payne. 2009. Energy pile test at Lambeth College, London: Geotechnical and thermodynamic aspects of pile response to heat cycles. Géotechnique, **59**(3): 237–248. https://doi.org/10.1680/geot.2009.59.3.237.

Brandl, H. 2006. Energy foundations and other thermo-active ground structures. Géotechnique, 56(2), 81-122. https://doi.org/10.1680/geot.2006.56.2.81.

Chen, Y., Xu, J., Li, H., Chen, L., Ng, CWW. and Liu, H. 2017. "Performance of a prestressed concrete pipe energy pile during heating and cooling". *J. Perform. Const. Fac.* 31 (3): 06017001. https://doi.org/10.1061/(ASCE)CF.1943-5509.0000982

Di Donna, A., Rotta Loria, A.F., and Laloui, L. 2016. Numerical study of the response of a group of energy piles under different combinations of thermo-mechanical loads. Computers and Geotechnics, **72**: 126-142. https://doi.org/10.1016/j.compgeo.2015.11.010.

Elzeiny, R., Suleiman, M. T., Xiao, S., Abu Qamar, M. A., and Al-Khawaja, M. 2020. Laboratory-scale pull-out tests on a geothermal energy pile in dry sand subjected to heating cycles. Canadian Geotechnical Journal. https://doi.org/10.1139/cgj-2019-0143.

Faizal, M., Bouazza, A., and Singh, R. M. 2016. An experimental investigation of the influence of intermittent and continuous operating modes on the thermal behaviour of a full scale geothermal energy pile. Geomechanics for Energy and the Environment, **8**: 8-29. https://doi.org/10.1016/j.gete.2016.08.001.

Faizal, M., Bouazza, A., Haberfield, C., and McCartney J.S. 2018. Axial and radial thermal responses of a field-scale energy pile under monotonic and cyclic temperature changes. Journal of Geotechnical and Geoenvironmental Engineering, **144**(10): 04018072. https://doi.org/10.1139/cgj-2018-0246.

Faizal, M., Bouazza, A., McCartney, J.S., and Haberfield, C. 2019a. Axial and radial thermal responses of an energy pile under a 6-storey residential building. Canadian Geotechnical Journal, **56**(7): 1019–1033. https://doi.org/10.1061/(ASCE)GT.1943-5606.0001952.

Faizal, M., Bouazza, A., McCartney, J. S., and Haberfield, C. 2019b. Effects of cyclic temperature variations on thermal response of an energy pile under a residential building. Journal of Geotechnical and Geoenvironmental Engineering, 145(10), 04019066.

Fang, J., Kong, G., Meng, Y., Wang, L., and Yang, Q. 2020. Thermomechanical behavior of energy piles and interactions within energy pile–raft foundations. Journal of Geotechnical and Geoenvironmental Engineering, 146(9), 04020079. https://doi.org/10.1061/(ASCE)GT.1943-5606.0002333.

Gawecka, K.A., Taborda, D.M.G., Potts, D.M., Cui, W., Zdravković, L., and Kasri, M.S.H. 2017. Numerical modelling of thermo-active piles in London Clay. Proceedings of the Institution of Civil Engineers - Geotechnical Engineering, **170**(3): 201-219.

Han, C., and Yu, X. B. 2020. Analyses of the thermo-hydro-mechanical responses of energy pile subjected to non-isothermal heat exchange condition. Renewable Energy. https://doi.org/10.1016/j.renene.2020.04.118.

Huang, X., Wu, Y., Peng, H., Hao, Y., and Lu, C. 2018. Thermomechanical behavior of energy pile embedded in sandy soil. Mathematical Problems in Engineering, 2018. https://doi.org/10.1155/2018/5341642.

Jeong, S., Lim, H., Lee, J.K., and Kim, J. 2014. Thermally induced mechanical response of energy piles in axially loaded pile groups. Applied Thermal Engineering, **71**(1): 608-615. https://doi.org/10.1016/j.applthermaleng.2014.07.007.

Liu, R. Y. W., Taborda, D. M. G., Gawecka, K. A., Cui, W., and Potts, D. M. 2019. Computational study on the effects of boundary conditions on the modelled thermally induced axial stresses in thermo-active piles. In Proceedings of the XVII ECSMGE-2019.

Olgun, C., Ozudogru, T., and Arson. 2014. Thermo-mechanical radial expansion of heat exchanger piles and possible effects on contact pressures at pile–soil interface. Géotechnique Letters, **4**(3): 170-178. https://doi.org/10.1680/geolett.14.00018.

Olgun, C. G., Ozudogru, T. Y., Abdelaziz, S. L., and Senol, A. 2015. Long-term performance of heat exchanger piles. Acta Geotechnica, **10**(5): 553-569. https://doi.org/10.1007/s11440-014-0334-z

Ozudogru, T.Y., Olgun, C.G., and Arson, C.F. 2015. Analysis of friction induced thermo-mechanical stresses on a heat exchanger pile in isothermal soil. Geotechnical and Geological Engineering, **33**(2): 357-371. https://doi.org/10.1007/s10706-014-9821-0.

McCartney, J.S., and Murphy, K.D. 2017. Investigation of potential dragdown/uplift effects on energy piles. Geomechanics for Energy and the Environment, **10**: 21-28. https://doi.org/10.1016/j.gete.2017.03.001.

Mimouni, T., and Laloui, L. 2015. Behaviour of a group of energy piles. Canadian Geotechnical Journal, **52**(12): 1913-1929. https://doi.org/10.1139/cgj-2014-0403.

Moradshahi, A., Faizal, M., Bouazza, A., and McCartney, J. S. 2020a. Effect of nearby piles and soil properties on the thermal behaviour of a field-scale energy pile. Canadian Geotechnical Journal. **0**(ja): -. https://doi.org/10.1139/cgj-2020-0353

Moradshahi, A., Khosravi, A., McCartney, J. S., and Bouazza, A. 2020b. Axial load transfer analyses of energy piles at a rock site. Geotechnical and Geological Engineering, **38**: 4711–4733. https://doi.org/10.1007/s10706-020-01322-5.Murphy, K.D., and McCartney, J.S. 2015. Seasonal response of energy foundations during building operation. Geotechnical and Geological Engineering, **33**(2): 343-356. https://doi.org/10.1007/s10706-014-9802-3.

Murphy, K.D., McCartney, J.S., and Henry, K. S. 2015. Evaluation of thermo-mechanical and thermal behavior of full-scale energy foundations. Acta Geotechnica, **10**(2): 179-195. https://doi.org/10.1007/s11440-013-0298-4.

Ng, C. W. W., and Ma, Q. J. 2019. Energy pile group subjected to non-symmetrical cyclic thermal loading in centrifuge. Géotechnique Letters, **9**(3), 173-177. https://doi.org/10.1680/jgele.18.00161

Pasten, C., and Santamarina, J. C. 2014. Thermally induced long-term displacement of thermoactive piles. Journal of Geotechnical and Geoenvironmental Engineering, 140(5), 06014003. https://doi.org/10.1061/(ASCE)GT.1943-5606.0001092.

Peck, R. B., Hanson, Walter E., and Thornburn, Thomas H. 1974. Foundation engineering (2nd ed.). Wiley.

Poulos, H.G., Mattes, N.S. 1985. Settlement and load distribution analysis of pile groups. In: Golden Jubilee of the International Society for Soil Mechanics and Foundation Engineering: Commemorative Volume. Institution of Engineers, Barton, Australia, p.155-165.

Ravera, E., Sutman, M. and Laloui, L. 2019. Analysis of the interaction factor method for energy pile groups with slab. Computers and Geotechnics, p.103294. https://doi.org/10.1016/j.compgeo.2019.103294.

Rotta Loria, A.F. and Laloui, L. 2016. The interaction factor method for energy pile groups. Computers and Geotechnics, **80**: 121-137. https://doi.org/10.1016/j.compgeo.2016.07.002.

Rotta Loria, A.F. and Laloui, L. 2017a. The equivalent pier method for energy pile groups. Géotechnique, **67**(8): 691–702. https://doi.org/10.1680/jgeot.16.P.139.

Rotta Loria, A.F. and Laloui, L. 2017b. Thermally induced group effects among energy piles. Géotechnique, **67**(5): 374-393. https://doi.org/10.1680/jgeot.16.P.039.

Rotta Loria, A. F. and Laloui, L. 2018. Group action effects caused by various operating energy piles. Géotechnique, **68**(9): 834-841. https://doi.org/10.1680/jgeot.17.P.213.

Rui, Y., and Soga, K. 2019. Thermo-hydro-mechanical coupling analysis of a thermal pile. Proceedings of the Institution of Civil Engineers-Geotechnical Engineering, 172(2), 155-173.

Saggu, R., and Chakraborty, T. 2016. Thermo-mechanical response of geothermal energy pile groups in sand. International Journal of Geomechanics, **16**(4): 04015100. https://doi.org/10.1061/(ASCE)GM.1943-5622.0000567.

Salciarini, D., Ronchi, F., Cattoni, E., and Tamagnini, C. 2015. Thermo-mechanical effects induced by energy piles operation in a small piled raft. International Journal of Geomechanics, **15**(2): 04014042. https://doi.org/10.1061/(ASCE)GM.1943-5622.0000375.

Salciarini, D., Ronchi, F., and Tamagnini, C. 2017. Thermo-hydro-mechanical response of a large piled raft equipped with energy piles: a parametric study. Acta Geotechnica, **12**(4): 703-728. https://doi.org/10.1007/s11440-017-0551-3.

Singh, R. M. and Bouazza, A. 2013. Thermal conductivity of geosynthetics. Geotextiles and Geomembranes, 39, 1-8.

Singh, R. M., Bouazza, A., and Wang, B. 2015. Near-field ground thermal response to heating of a geothermal energy pile: Observations from a field test. Soils and Foundations, 55(6), 1412-1426.

Sung, C., Park, S., Lee, S., Oh, K., and Choi, H. 2018. Thermo-mechanical behavior of cast-in-place energy piles. Energy, **161**: 920-938. https://doi.org/10.1016/j.energy.2018.07.079.

Suryatriyastuti, M.E., Mroueh, H., and Burlon, S. 2012. Understanding the temperature-induced mechanical behaviour of energy pile foundations. Renewable and Sustainable Energy Reviews, **16**(5): 3344-3354. https://doi.org/10.1016/j.rser.2012.02.062.

Suryatriyastuti, M.E., Burlon, S., and Mroueh, H. 2016. On the understanding of cyclic interaction mechanisms in an energy pile group. International Journal for Numerical and Analytical Methods in Geomechanics, 40(1): 3-24. https://doi.org/10.1002/nag.2382.

Wang, B., Bouazza, A., Singh, R.M., Haberfield, C., Barry-Macaulay, D., and Baycan, S. 2015. Posttemperature effects on shaft capacity of a full-scale geothermal energy pile. Journal of Geotechnical and Geoenvironmental Engineering, **141**(4): 04014125. https://doi.org/10.1061/(ASCE)GT.1943-5606.0001266.

Wu, D., Liu, H., Kong, G., and Ng, C.W.W. 2020. Interactions of an energy pile with several traditional piles in a row. Journal of Geotechnical and Geoenvironmental Engineering, **146**(4). https://doi.org/10.1061/(ASCE)GT.1943-5606.0002224.

Yang, W., Zhang, L., Zhang, H., Wang, F., and Li, X. 2020. Numerical investigations of the effects of different factors on the displacement of energy pile under the thermo-mechanical loads. Case Studies in Thermal Engineering, 100711. https://doi.org/10.1016/j.csite.2020.100711.

Yavari, N., Tang, A. M., Pereira, J. M., and Hassen, G. 2014. Experimental study on the mechanical behaviour of a heat exchanger pile using physical modelling. Acta Geotechnica, **9**(3), 385-398. https://doi.org/10.1007/s11440-014-0310-7.

You, S., Cheng, X., Guo, H., and Yao, Z. 2014. In-situ experimental study of heat exchange capacity of CFG pile geothermal exchangers. Energy and Buildings, **79**: 23-31. https://doi.org/10.1016/j.enbuild.2014.04.021.

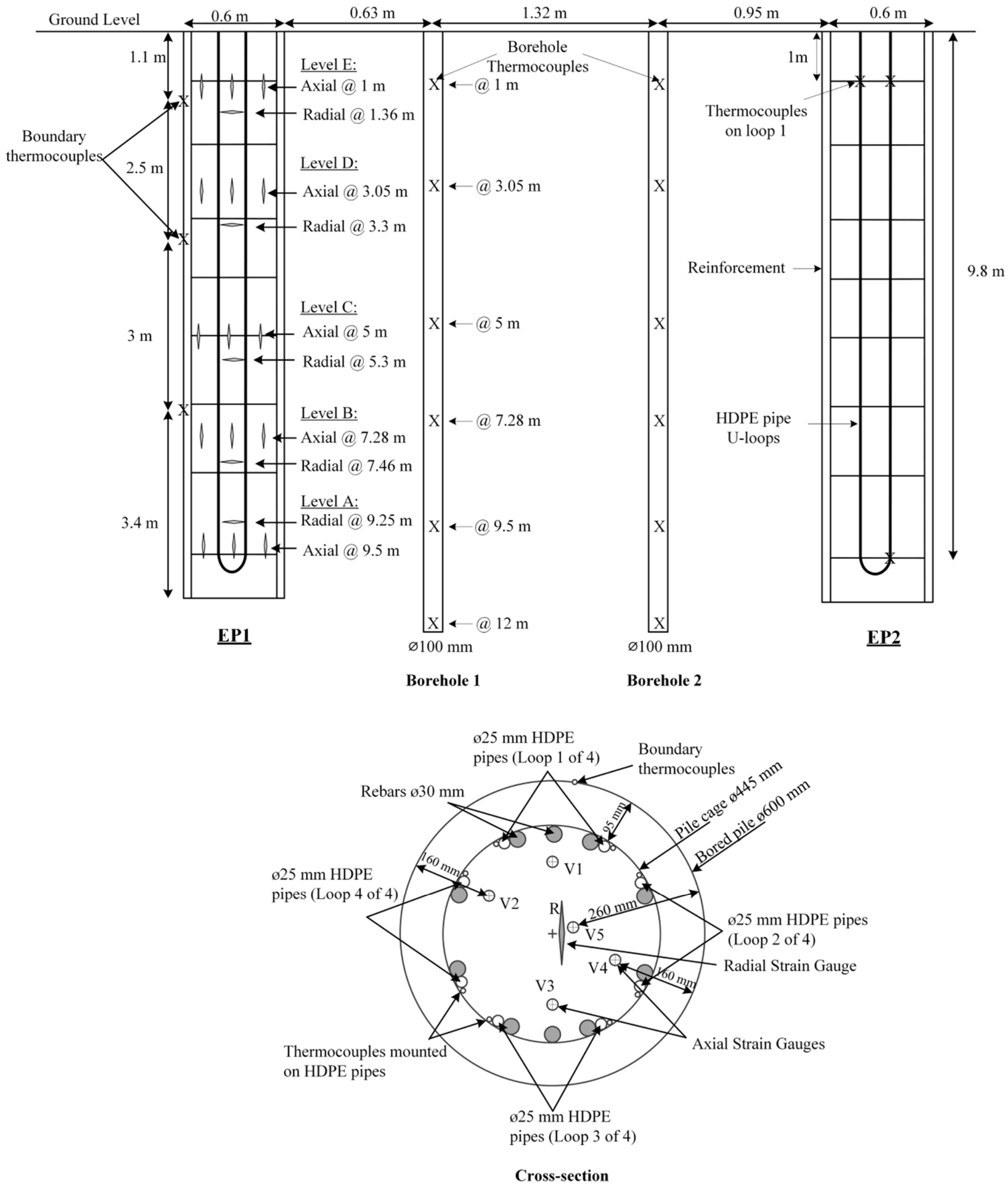

Figure 1. Details of the field-scale energy piles(Faizal et al., 2019; Moradshahi et al., 2020a).

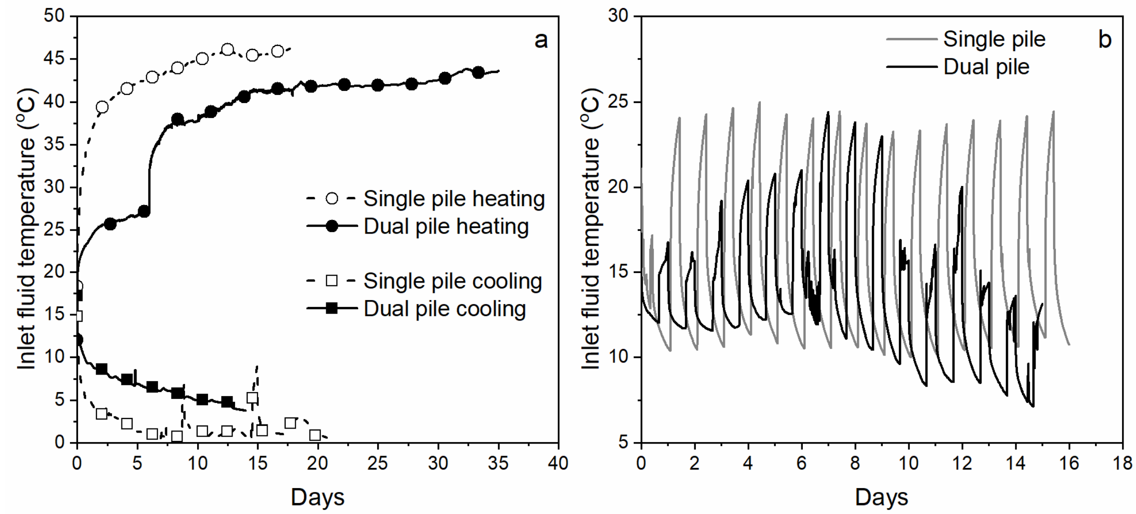

Figure 2. Experimental fluid temperatures for (a) monotonic heating and cooling and (b) cyclic heating and cooling.

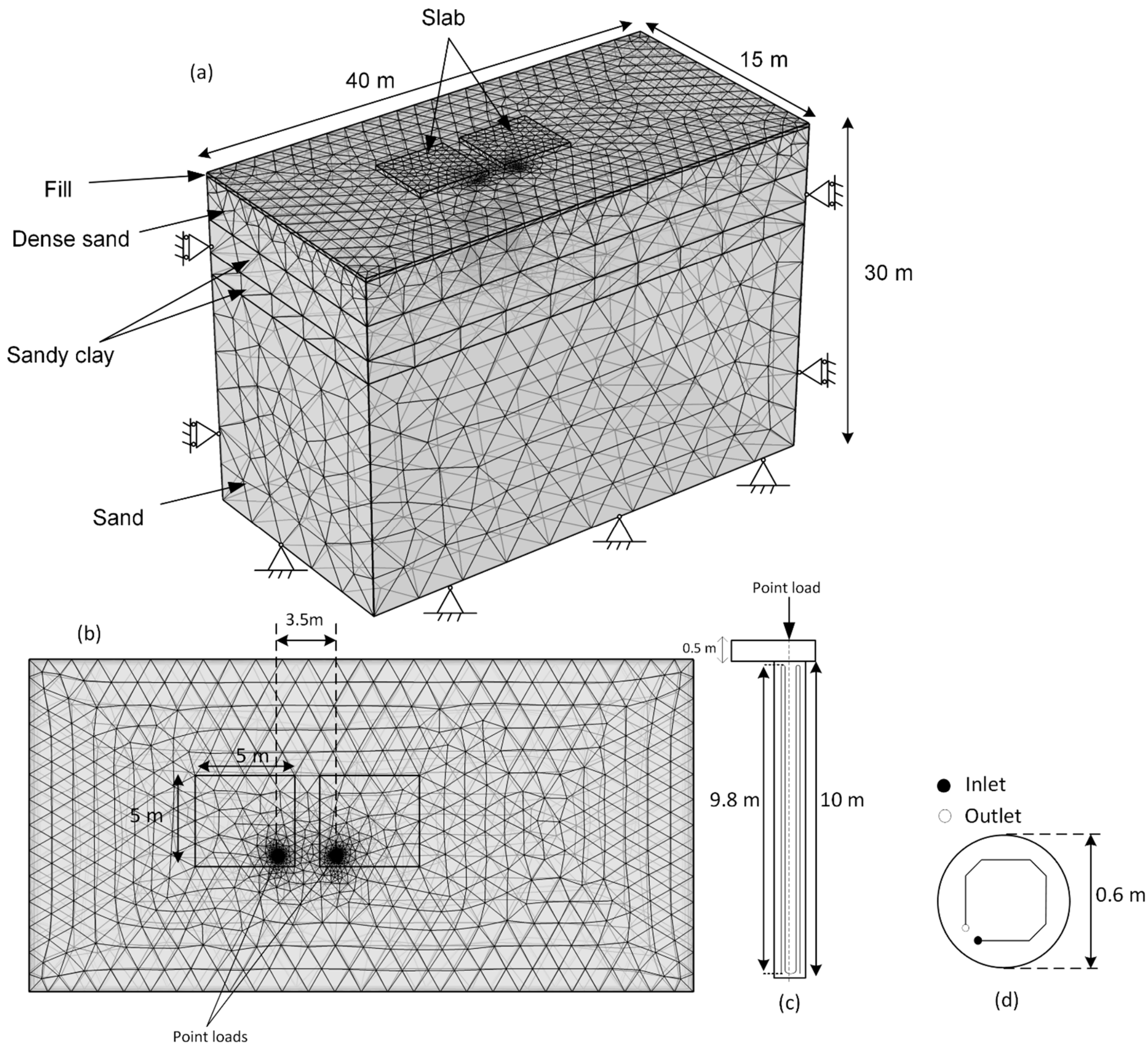

Figure 3. Finite element mesh of the numerical model (a) 3D view; (b) plan view; (c) side view of each energy pile with internal heat exchanger loops; and (d) plan view of energy pile showing connection of the four heat exchanger loops at the pile head. (after Moradshahi et al. 2020a)

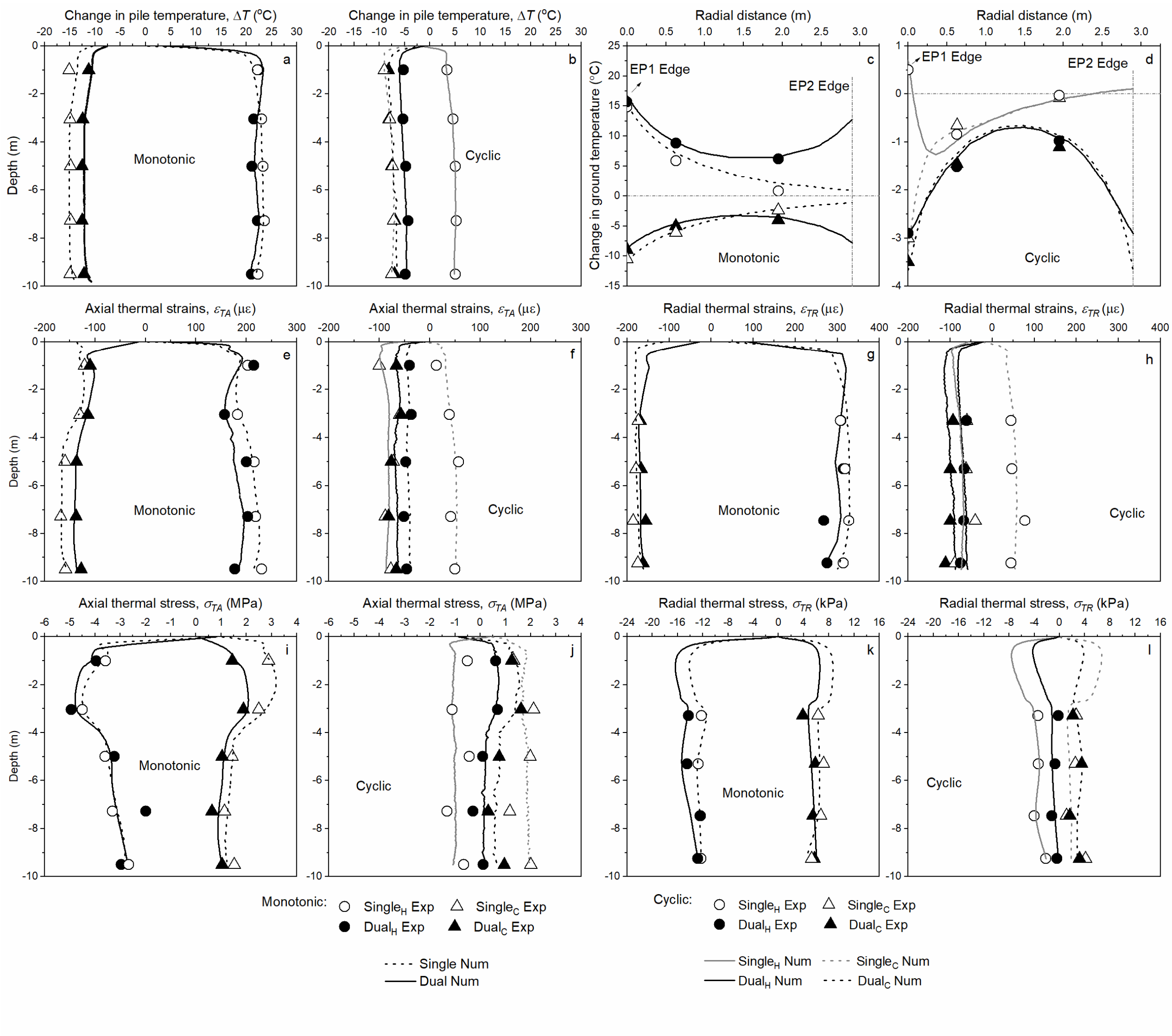

Figure 4. Experimental and numerical profiles in EP1 of: (a) and (b): ΔT during monotonic and cyclic temperatures, respectively; (c) and (d): ΔT of ground at depth of 5 m during monotonic and cyclic temperatures, respectively; (e) and (f) ε_{TA} during monotonic and cyclic temperatures, respectively; (g) and (h) ε_{TR} during monotonic and cyclic temperatures, respectively; (i) and (j) σ_{TA} during monotonic and cyclic temperatures, respectively; (k) and (l) σ_{TR} during monotonic temperatures and cyclic temperatures, respectively.

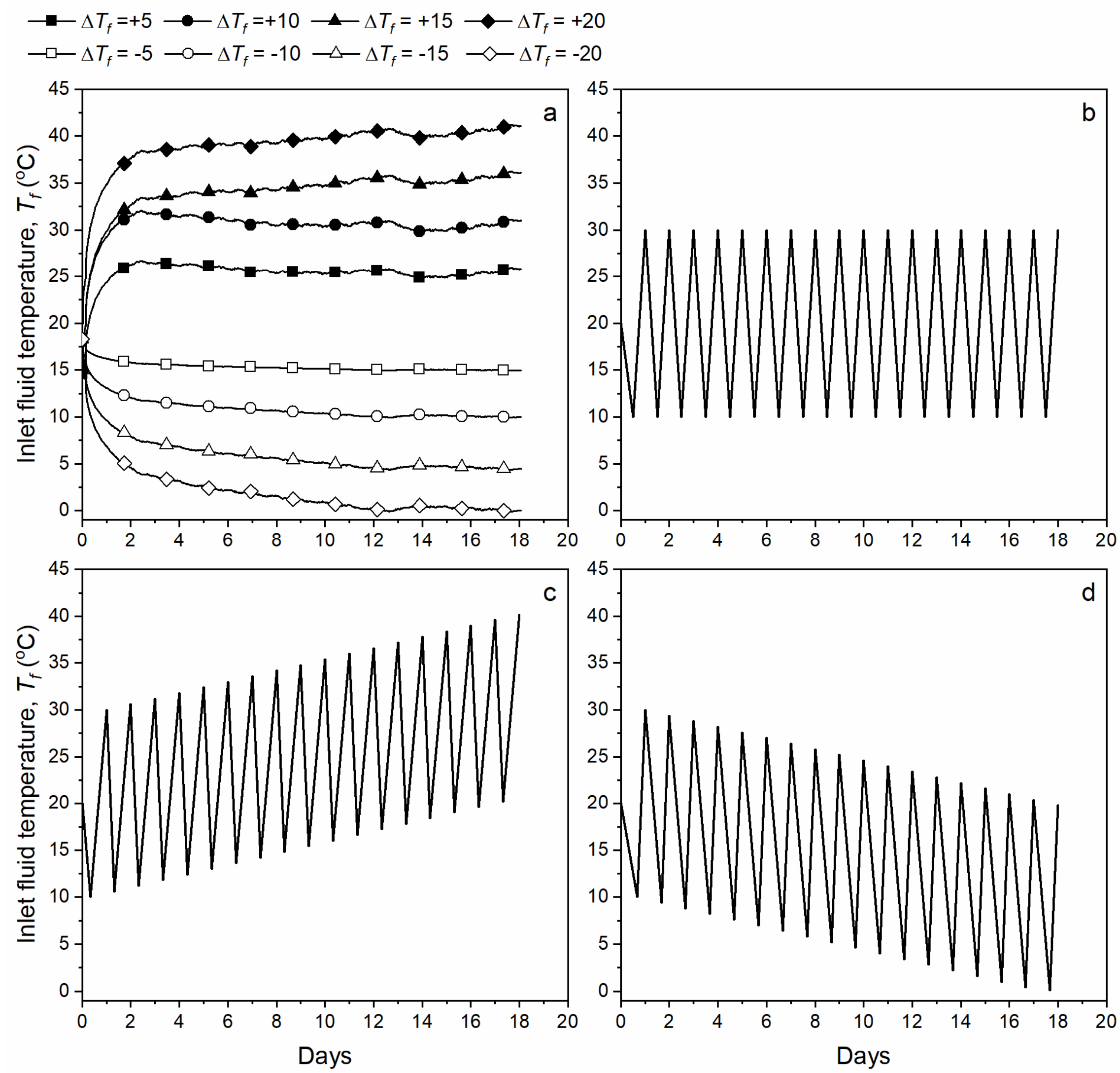

Figure 5. Inlet fluid temperatures (a) monotonic heating and cooling; (b) balanced cyclic; (c) heating oriented imbalanced cyclic; and (d) cooling oriented imbalanced cyclic fluid temperature for the parametric study.

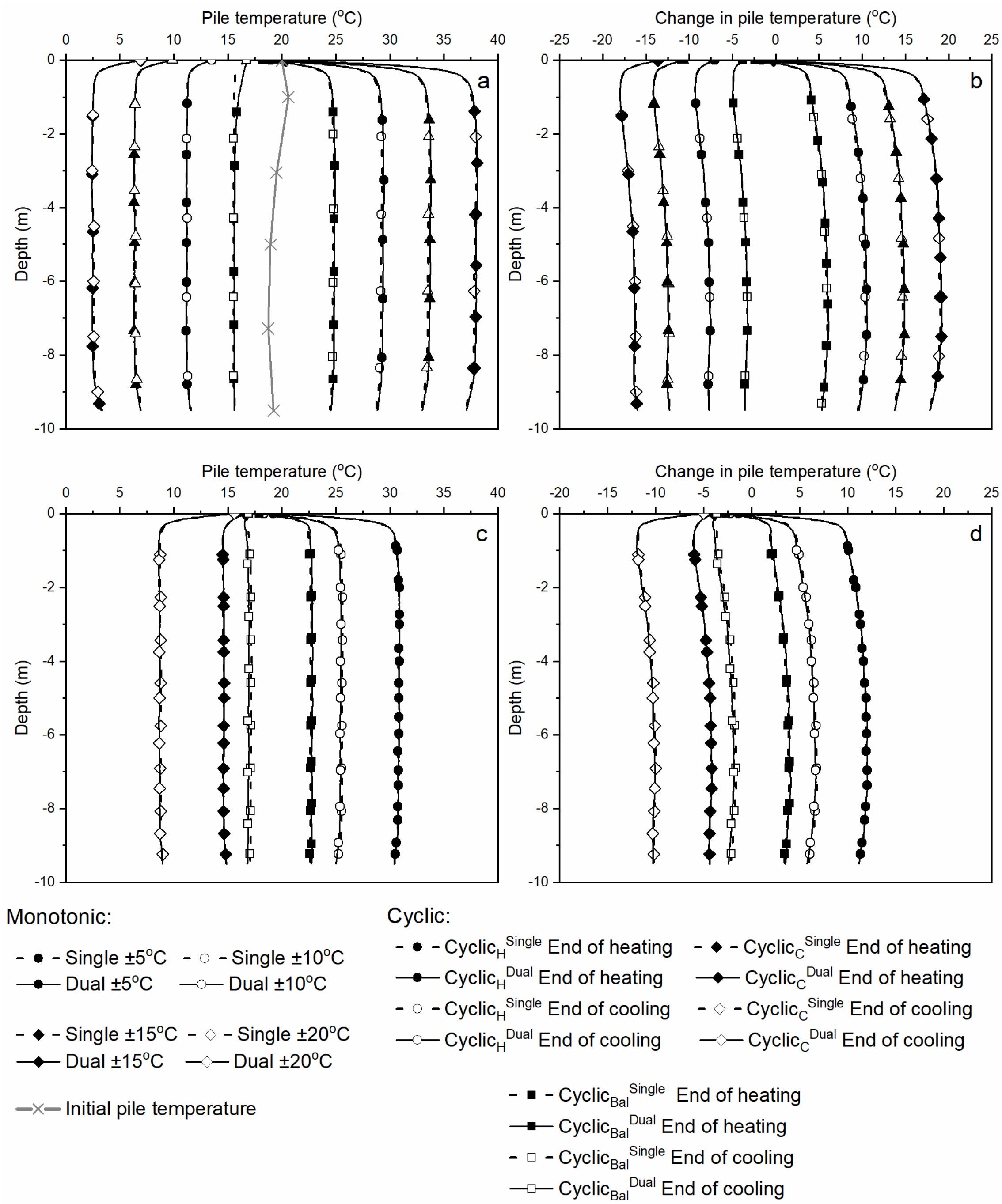

Figure 6. Numerical predictions of temperature and change in temperatures in EP1: (a) and (b) temperature and change in pile temperature for monotonic heating and cooling; (c) and (d) temperature and change in pile temperature for cyclic operation.

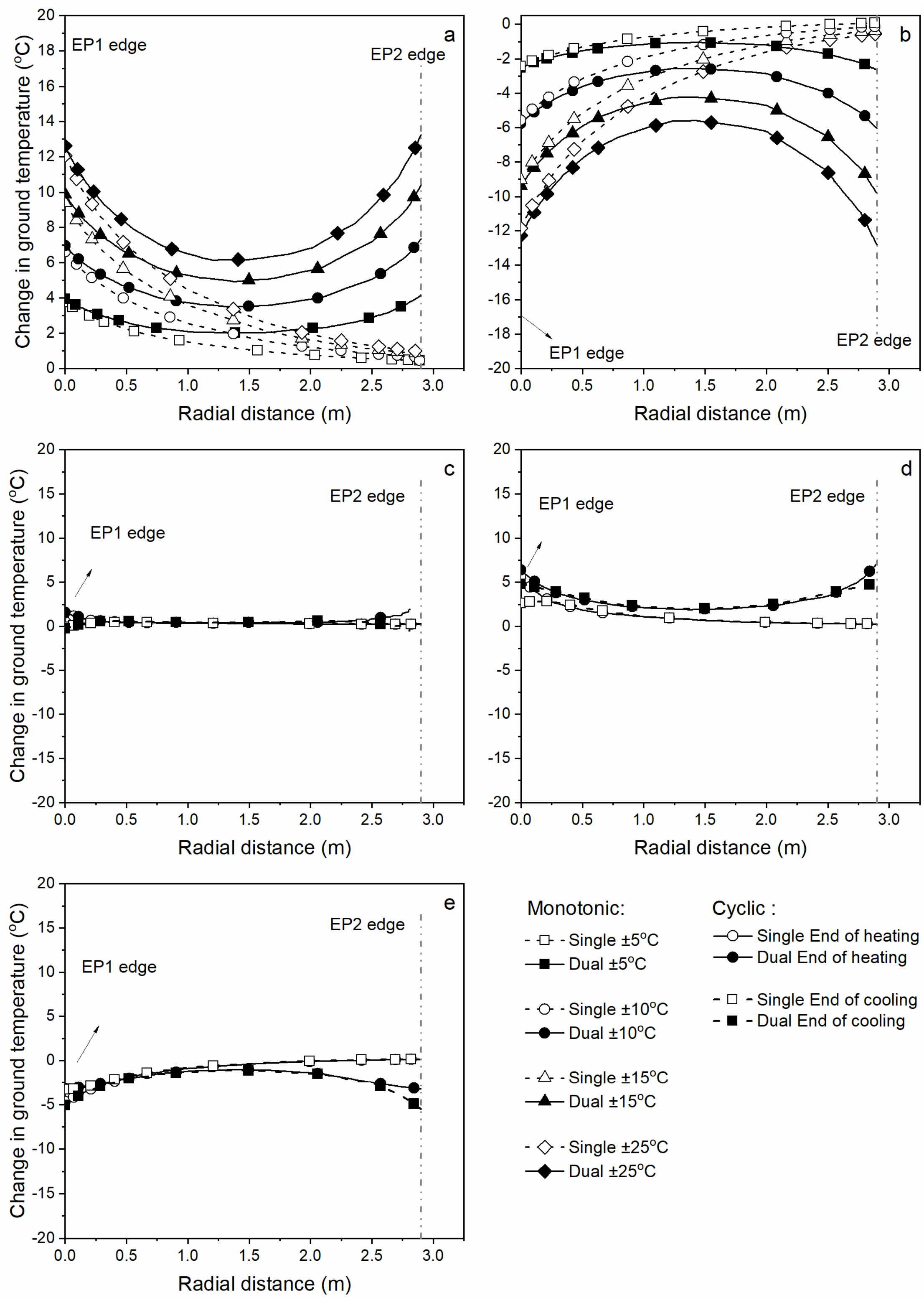

Figure 7. Numerical prediction of ground temperature distributions between the piles: (a) monotonic heating; (b) monotonic cooling; (c) balanced cyclic temperatures; (d) heating oriented imbalanced cyclic temperatures; and (e) cooling oriented imbalanced cyclic temperatures

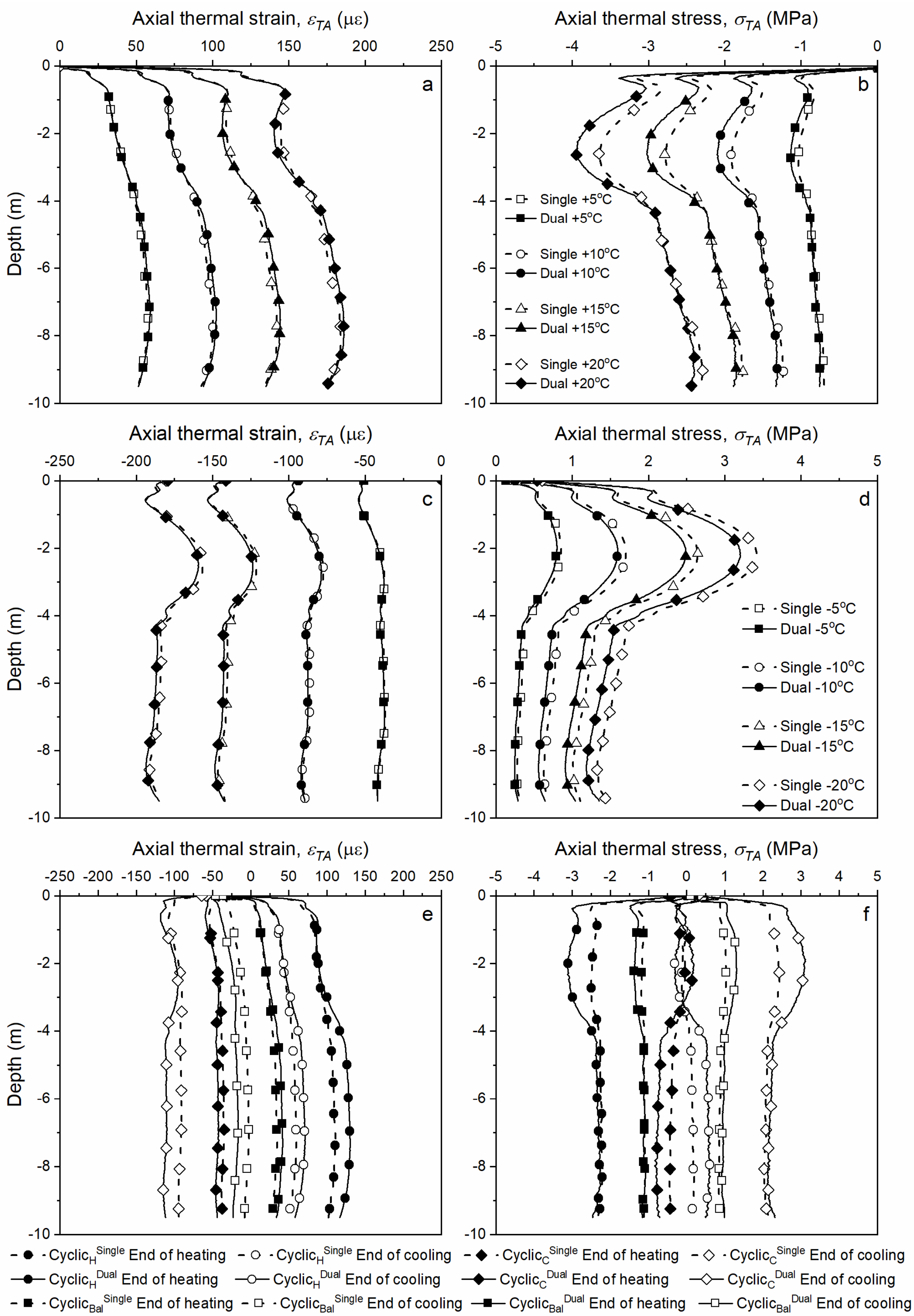

Figure 8. Numerical axial thermal responses of EP1: (a) and (b), strains and stresses at the end of monotonic heating; (c) and (d), strains and stresses at the end of monotonic cooling; (e) and (f), strains and stresses for the last cycle of cyclic operations.

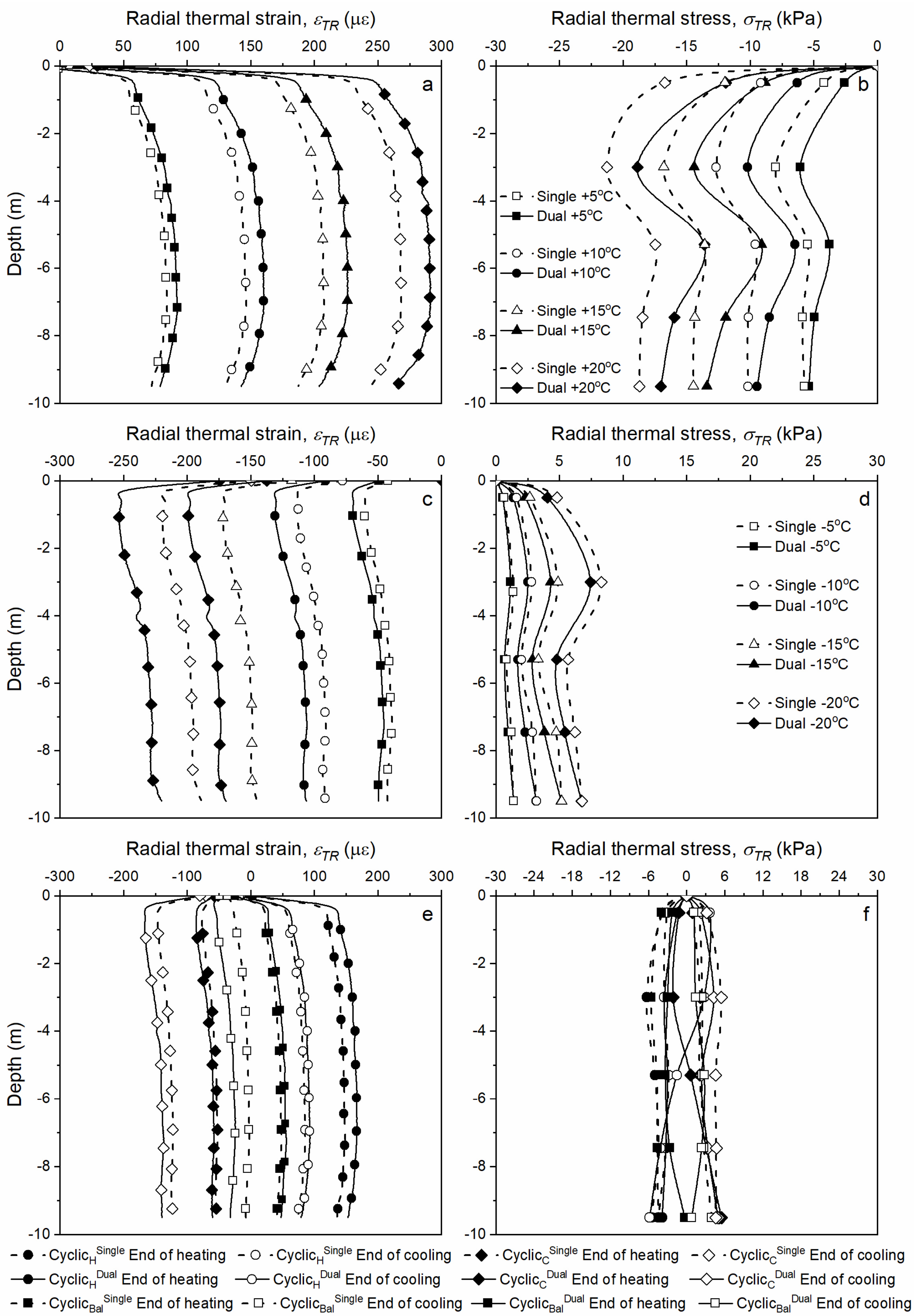

Figure 9. Numerical prediction of radial thermal responses in EP1: (a) and (b), strains and stresses at the end of monotonic heating; (c) and (d), strains and stresses at the end of monotonic cooling; (e) and (f), strains and stresses for the last cycle of cyclic operations.

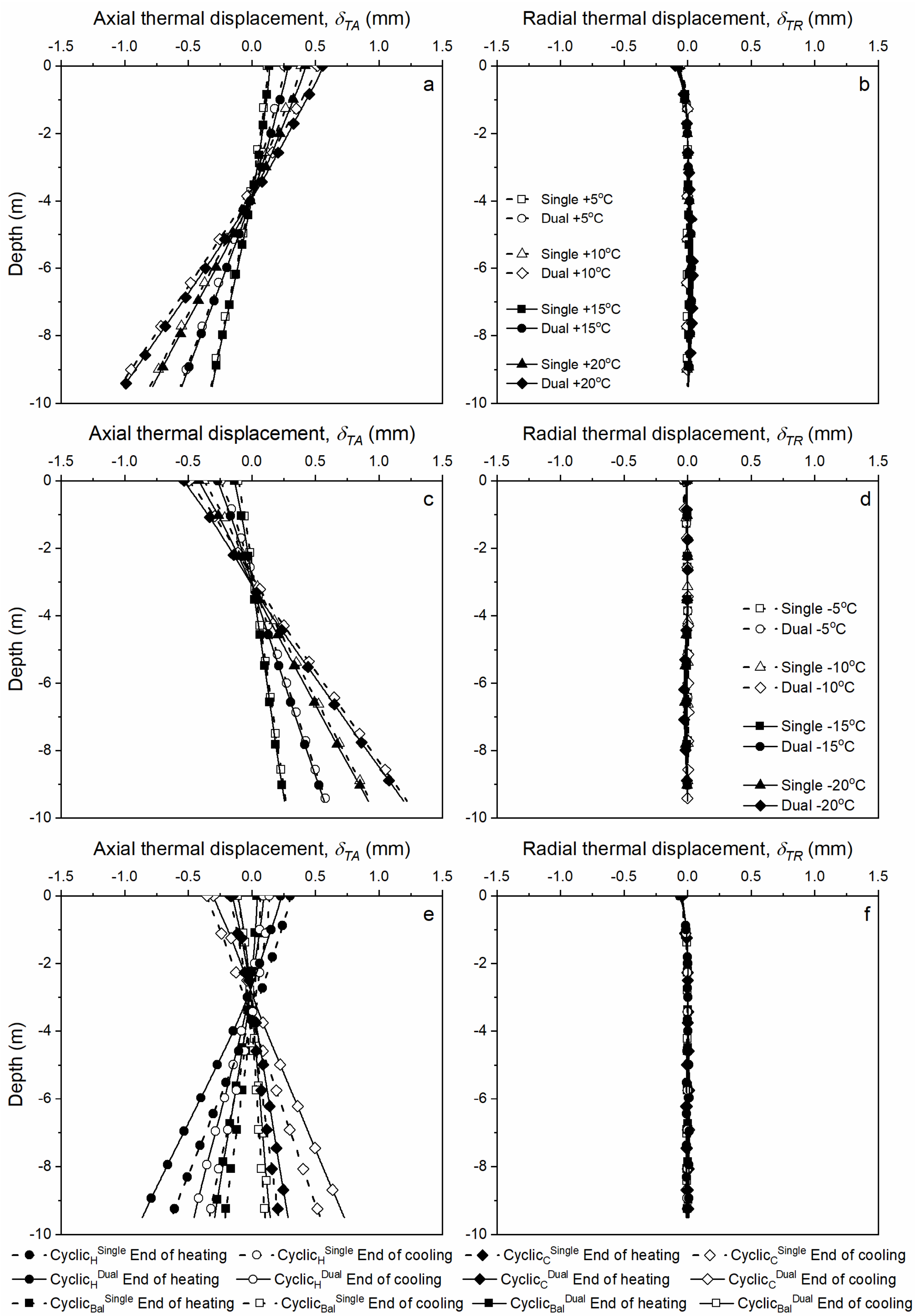

Figure 10. Numerical prediction of axial (δ_{TA}) and radial (δ_{TR}) displacements of EP1: (a) and (b) δ_{TA} and δ_{TR} for monotonic heating; (c) and (d) δ_{TA} and δ_{TR} for monotonic cooling; (e) and (f) δ_{TA} and δ_{TR} for the last cycle of cyclic operations.

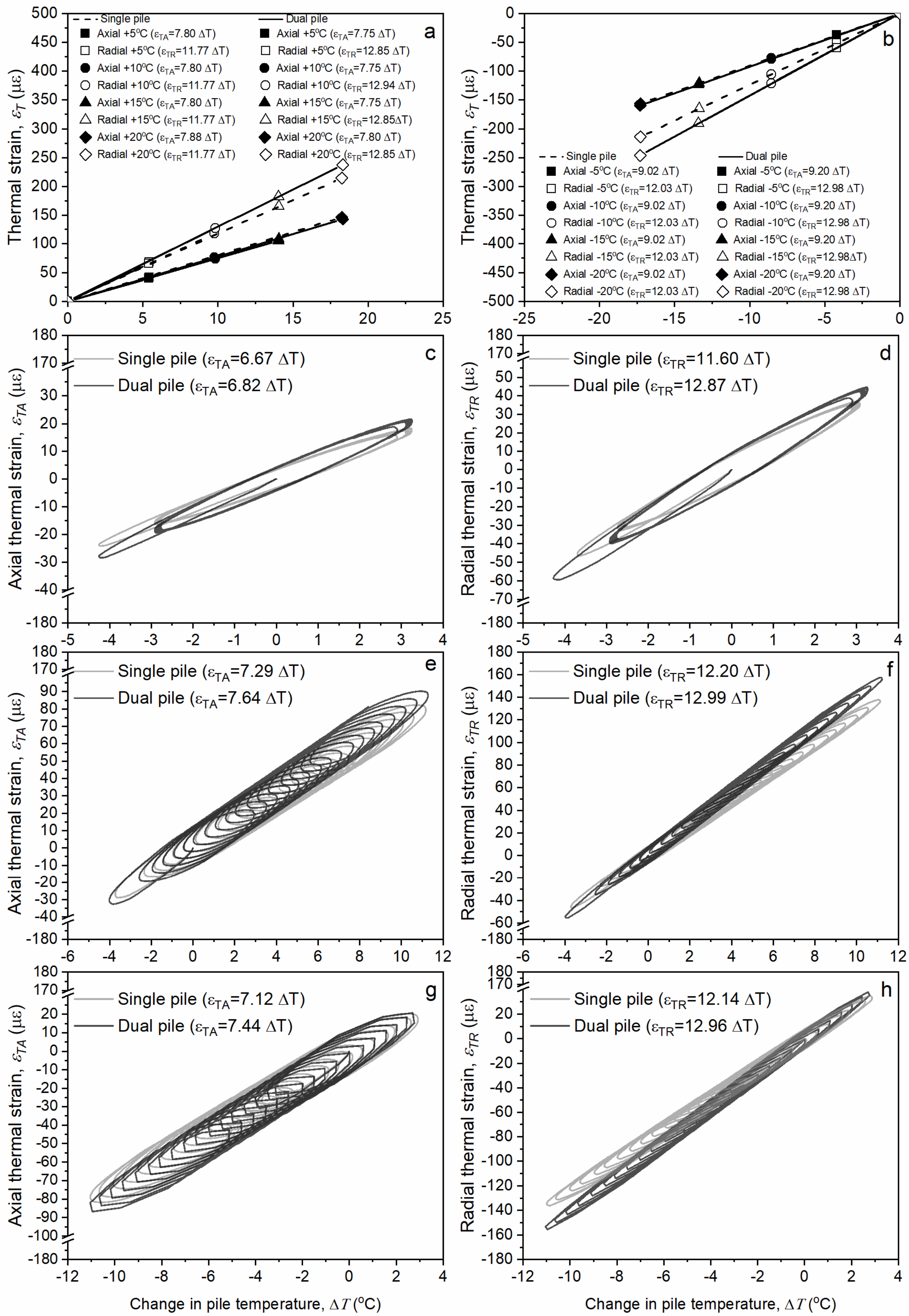

Figure 11. Numerical prediction of axial (ε_{TA}) and radial (ε_{TR}) thermal strains against change in pile temperatures at a depth of 2.6 m near the null point: (a) monotonic heating; (b) monotonic cooling; (c) and (d) ε_{TA} and ε_{TR} for balanced cyclic, respectively; (e) and (f) ε_{TA} and ε_{TR} for heating oriented imbalanced cyclic, respectively; and (g) and (h) ε_{TA} and ε_{TR} for cooling oriented imbalanced cyclic.

Table 1. Material properties for numerical simulations calibrated against field test measurements.

Soil properties	Fill	Dense sand	Sandy clay	Sand	Pile	Slab	HDPE pipes
Depth, z (m)	0.0-0.5	0.5-3.5	3.5-6.0	6.0-12.5	1750	800	—
Elastic modulus, E (MPa)	15	600	75	120	35000	35000	—
Poisson's ratio, ν (—)	0.30	0.28	0.30	0.30	0.22	0.22	—
Total density, ρ (kg/m^3)	1750	1800	1950	2200	2200	850	—
Specific heat capacity, C_p (J/kg°C)	800	840	810	850	810	850	—
Thermal conductivity, λ (W/(m°C))	1.1	1.7	2.0	2.3	1.5	1.5	0.4
Linear coefficient of thermal expansion, α (με/°C)	10	10	10	10	13	13	—
Friction angle (degrees)	30	38	32	35	—	—	—
Apparent cohesion (kPa)	1	0.1	0.2	0.1	—	—	—

Table 2. Description of experiments

Operation mode	Description	Inlet water temperature (°C)	Inlet water flow rates (L/min)	Experiment duration (Days)
Single heating	24 h of heating (Faizal et al., 2019a)	46	11	18
Dual heating	24 h of heating	42	10	42
Single cooling	24 h of cooling	1	12	21
Dual cooling	24 h of cooling	5	10	14
Single cyclic	16 h cooling and 8 h heating (Faizal et al., 2019b)	8-26	16	16
Dual cyclic	16 h cooling and 8 h heating	4-25	14	15